Lineage tracing of neuromesodermal progenitors reveals novel Wnt-dependent roles in trunk progenitor cell maintenance and differentiation

Robert J. Garriock, Ravindra B. Chalamalasetty, Mark W. Kennedy, Lauren C. Canizales, Mark Lewandoski and Terry P. Yamaguchi*

ABSTRACT

In the development of the vertebrate body plan, Wnt3a is thought to promote the formation of paraxial mesodermal progenitors (PMPs) of the trunk region while suppressing neural specification. Recent lineage-tracing experiments have demonstrated that these trunk neural progenitors and PMPs derive from a common multipotent progenitor called the neuromesodermal progenitor (NMP). NMPs are known to reside in the anterior primitive streak (PS) region; however, the extent to which NMPs populate the PS and contribute to the vertebrate body plan, and the precise role that Wnt3a plays in regulating NMP self-renewal and differentiation are unclear. To address this, we used cell-specific markers (Sox2 and T) and tamoxifen-induced Cre recombinase-based lineage tracing to locate putative NMPs *in vivo*. We provide functional evidence for NMP location primarily in the epithelial PS, and to a lesser degree in the ingressed PS. Lineage-tracing studies in Wnt3a/β-catenin signaling pathway mutants provide genetic evidence that trunk progenitors normally fated to enter the mesodermal germ layer can be redirected towards the neural lineage. These data, combined with previous PS lineage-tracing studies, support a model that epithelial anterior PS cells are Sox2$^+$T$^+$ multipotent NMPs and form the bulk of neural progenitors and PMPs of the posterior trunk region. Finally, we find that Wnt3a/β-catenin signaling directs trunk progenitors towards PMP fates; however, our data also suggest that Wnt3a positively supports a progenitor state for both mesodermal and neural progenitors.

KEY WORDS: Neural progenitor, Neuromesodermal progenitor, Wnt signaling, Brachyury, Paraxial mesoderm, Sox2

INTRODUCTION

How progenitor populations are directed to differentiate into different cell lineages is poorly understood *in vivo*, particularly for the embryonic progenitors of the neural and mesodermal lineages. Neuroectoderm and mesoderm progenitors were originally thought to arise as separate descendants of the pluripotent epiblast during early gastrulation (Bellairs, 1986; Garcia-Martinez and Schoenwolf, 1992; Tam and Behringer, 1997). However, in mammalian embryos, a common neuromesodermal progenitor (NMP) is thought to give rise to both neural and paraxial mesoderm progenitors (PMPs) (Cambray and Wilson, 2002, 2007; Tam and Beddington, 1987; Tzouanacou et al., 2009; Wilson et al., 2009). The descendants of the neural

Center for Cancer Research, Cancer and Developmental Biology Laboratory, Cell Signaling in Vertebrate Development Section, NCI-Frederick, NIH, Frederick, MD 21702, USA.

*Author for correspondence (yamagute@mail.nih.gov)

progenitors give rise to the spinal cord, whereas the PMPs can differentiate into bone, cartilage, muscle, dermis and connective tissue. Thus, the potential of NMPs is remarkable, perhaps accounting for the majority of tissues that form the trunk and tail.

Multipotent progenitors have been identified in the mouse primitive streak (PS) region near the embryonic node by cell-tracing experiments showing that individual or groups of progenitors give rise to both neural and paraxial mesoderm (PM) (Cambray and Wilson, 2002, 2007; Tzouanacou et al., 2009; Wilson et al., 2009). Regional PS progenitors show the capacity to contribute to multiple cell types along the body axis and can be passaged through multiple successive host embryos, suggesting that the PS region contains stem cell populations (Cambray and Wilson, 2002; Wilson et al., 2009). However, recognizing axial stem cells *in vivo* by molecular criteria remains a challenge as the PS region is a site of dynamic and continuous cell movement with different, indistinguishable populations of cells entering, exiting and residing in the PS (Garcia-Martinez and Schoenwolf, 1992; Schoenwolf et al., 1992; Wilson and Beddington, 1996). NMPs are proposed to co-express Sox2, a pluripotency and neural progenitor marker, and the PS marker T, also known as brachyury (Martin and Kimelman, 2012; Wilson et al., 2009). Although Sox2/T co-expressing regions have been documented in the PS region in mammals (Tsakiridis et al., 2014), no study has demonstrated that Sox2/T co-expression functionally represents multipotent NMPs.

One way to address whether T-expressing cells include NMPs is to take a gene-specific transgenic lineage-tracing approach. The recently developed *TCreERT2* transgenic line, in which the tamoxifen (TAM)-inducible CreERT2 recombinase is driven by the *T* promoter, has the potential to trace NMPs *in vivo* as it is expressed in the anterior epithelial PS region where NMPs are thought to exist (Anderson et al., 2013; Wilson et al., 2009). *TCreERT2* also has the advantage of excluding pluripotent epiblast stem cells that are capable of giving rise to most embryonic cell types, including neural and mesodermal cells. Previous transgenic tracing experiments have successfully used TAM-inducible Cre-based transgenics to follow the population dynamics of diverse progenitor populations *in vivo* (Boyle et al., 2008; Göthert et al., 2005; Masahira et al., 2006; Schepers et al., 2012; Srinivasan et al., 2007).

Wnt3a has been proposed to be a crucial regulator of NMP maintenance and differentiation, and presumably does so through β-catenin/Tcf transcriptional complexes and the subsequent activation of downstream target genes (Clevers and Nusse, 2012) such as *T* (Yamaguchi et al., 1999). In the absence of *Wnt3a* or *T*, the embryo fails to generate the posterior-most ∼55 of 65 skeletal elements/vertebrae, resulting in a severe posterior axis truncation (Herrmann, 1992; Takada et al., 1994). The loss of

skeletal elements corresponds to a reduction in progenitor markers, indicating a collapse in the progenitor populations that build the embryonic trunk (Yamaguchi et al., 1999). Importantly, *Wnt3a*, *Tcf1;Lef1* double mutants, and *T* mutant embryos show an expansion of neural tissue in the form of an ectopic neural tube, giving support to the hypothesis that the Wnt3a/β-catenin/Tcf1-Lef1/T axis is directly regulating the differentiation of NMPs into neural or mesodermal progenitors (Galceran et al., 1999; Herrmann, 1992; Yamaguchi et al., 1999; Yoshikawa et al., 1997). Single cell studies in zebrafish further this argument by showing that embryonic progenitors will selectively form striated skeletal muscle tissue when exposed to high Wnt signaling and, by contrast, form neural tissue when Wnt signaling is inhibited (Martin and Kimelman, 2012). From these, and other studies, a model of Wnt3a function has evolved to incorporate the concept of the NMP (Fig. 1A) (Galceran et al., 1999; Li and Storey, 2011; Martin and Kimelman, 2008, 2012; Takada et al., 1994; Yamaguchi et al., 1999; Yoshikawa et al., 1997). This model predicts that Wnt has a direct role in NMP maintenance, inducing PM cell fate and repressing neural cell fate. However, the model remains hypothetical and has not been directly tested in the native mammalian niche. The *Wnt3a*-null and conditional *Ctnnb1* (β-catenin) mouse mutants provide excellent opportunities to study NMP behavior *in vivo* as the fate of these cells can be dramatically modulated through these single gene mutations.

Here, we show that Wnt3a is required for regulating the balance of PM and neural tissues through the regulation of progenitor populations located at the posterior pole of the extending anterior-posterior axis. We further show that Wnt3a/β-catenin signals play a key role in maintaining Sox2$^+$T$^+$ NMPs and, unexpectedly, do not repress neural fates.

RESULTS

Imbalance of neural progenitors and PMPs, and differentiated descendants in *Wnt3a*$^{-/-}$ mutants

To assess neural progenitors and PMPs in *Wnt3a*$^{-/-}$ mutants, we examined representative markers of each population in sections taken just posterior to the forelimb, corresponding to the level of the 13th-16th somite (s13-16) of wild-type E9.5 embryos. Phenotypic differences are clearly evident between control and *Wnt3a*$^{-/-}$ mutant embryos at this stage and axial level (Takada et al., 1994; Yoshikawa et al., 1997). E9.5 *Wnt3a*$^{-/-}$ mutant embryos showed enlarged and malformed neural tissue evident by detection of the neural progenitor marker Sox2, while fibronectin expression revealed a reduced PM (Fig. 1B). Quantification showed that *Wnt3a*$^{-/-}$ mutants had significantly more neural progenitors and fewer
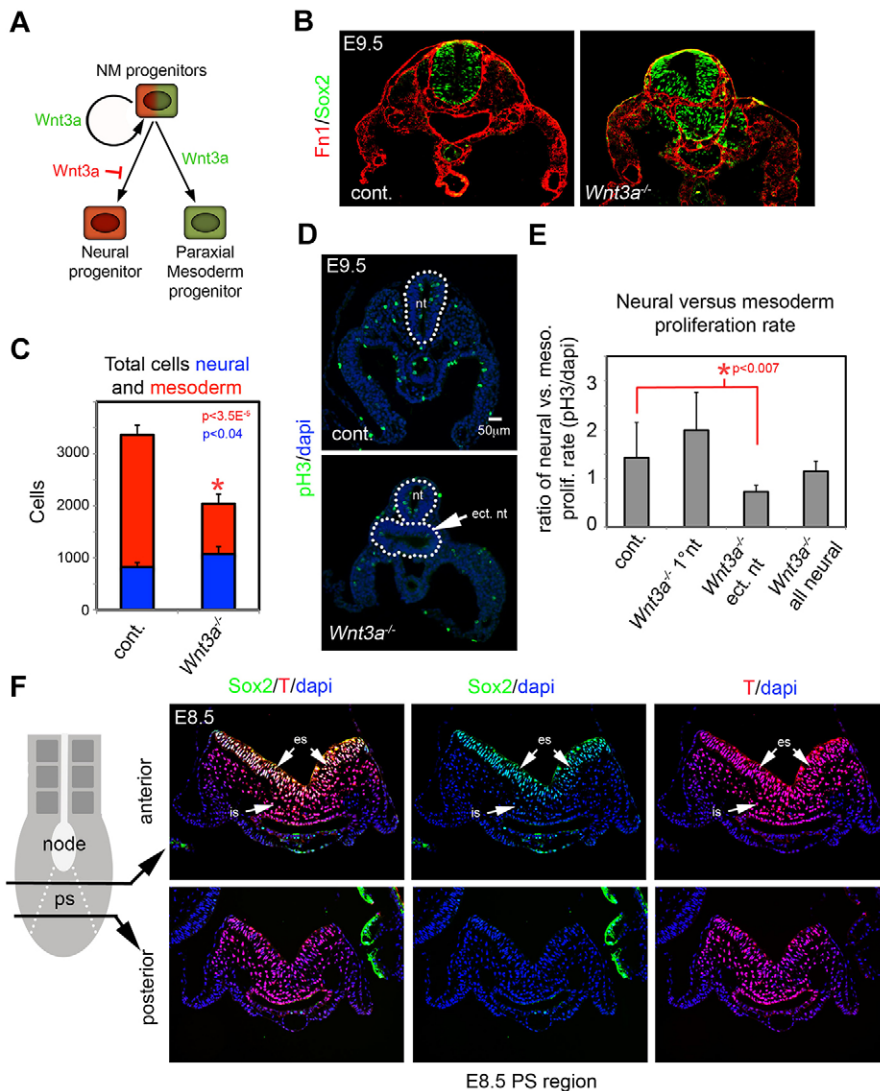

Fig. 1. Loss of PMPs and expansion of neural progenitors in *Wnt3a*$^{-/-}$ mutants is not due to changes in cell proliferation. (A) Proposed model of Wnt3a function in NMPs. Wnt3a maintains NMPs and promotes PM differentiation while inhibiting neural differentiation. (B) Detection of Sox2 (neural progenitors) and fibronectin (Fn1) (mesodermal mesenchyme) in the s13-16 region of E9.5 control and *Wnt3a*$^{-/-}$ embryos. (C) Graph of total cell counts of neural and mesodermal cells at E9.5 (n=4 control, n=5 *Wnt3a*$^{-/-}$). Data are mean±s.e.m. P<3.5×10^{-5} (mesoderm) and P<0.04 (neural), Student's t-test. (D) Detection of proliferating cells in E9.5 trunk region of control and *Wnt3a*$^{-/-}$ embryos by phospho-histone H3 detection. Dotted line indicates the neural tube(s). (E) Graph of neural versus mesodermal proliferation rate in control and *Wnt3a*$^{-/-}$ embryo at E9.5. Data are mean±s.e.m. P<0.007, Student's t-test. (F) Detection of Sox2 and T at E8.5 in sections taken through anterior and posterior regions of the PS. es, epithelial PS; is, ingressed PS; nt, neural tube; ect. nt, ectopic neural tube.

mesodermal cells than control embryos (Fig. 1C). At later stages of development, this phenotype manifests itself as a malformed neural tube and loss of musculoskeletal tissues, among others (supplementary material Fig. S1).

Although the observed progenitor imbalance can be explained by fate changes of NMPs, Wnt-dependent differential progenitor growth could also account for the phenotype. For example, Wnt3a could act to promote mesodermal growth and inhibit neural progenitor growth. To test this, we examined the cell proliferation rates of differentiating neural and mesodermal cells by detection of p-Histone H3 (Fig. 1D). The rate of cell proliferation was not significantly different in neural versus mesodermal populations, comparing littermate control embryos with $Wnt3a^{-/-}$ mutants, despite the apparent loss of PM tissue and an increase in neural tissue in $Wnt3a^{-/-}$ mutants at E9.5 (Fig. 1C; supplementary material Fig. S1). The only significant difference was the proliferation rate of the ectopic neural tissue in $Wnt3a^{-/-}$ mutants, which was lower than controls in or in $Wnt3a^{-/-}$ primary neural tube (Fig. 1E). We also observed no difference in neural versus mesodermal proliferation rates between control and $Wnt3a^{-/-}$ mutants in the E8.5 trunk region (supplementary material Fig. S1). These data suggest that differential neural and mesodermal growth is insufficient to explain the Wnt3a-dependent progenitor imbalance.

Detection of Sox2 and T co-expressing cells in the primitive streak

The PS is the source of progenitors for the trunk region during the extension of the body axis. In $Wnt3a^{-/-}$ mutants, changes in the fate of NMPs residing in the streak are presumably responsible for the observed imbalances in neural and mesodermal cell types in the trunk. To localize these putative NMPs by immunohistochemistry in wild-type embryos at E8.5, we used antibodies to Sox2 and T that are thought to mark the NMP. Sox2 was detected in the epithelial PS and, to a much lower degree, in ingressed cells of anterior, but not posterior, regions of the PS. T was strongly expressed in the epithelial and the ingressed regions of the PS along the anterior-posterior (A-P) extent of the PS. Co-detection of Sox2 and T was primarily observed in the epithelial PS, and to a lesser degree in ingressed cells (Fig. 1F), but was not observed near the notochord/node transition, where Sox2 and T marked distinct cell populations (supplementary material Fig. S1). Although our data indicate zones of putative NMPs, it is unclear whether these $Sox2^+T^+$ populations retain the potential to give rise to both neural and mesodermal cells.

Tracing trunk progenitors *in vivo* using a TAM-inducible *TCreERT2* transgene

To study the fate of potential NMPs, we crossed the conditional TAM-inducible transgenic line, *TCreERT2* (Anderson et al., 2013), to the *R26R-lacZ* Cre reporter line (Soriano, 1999) to permanently label T^+ PS cells with β-Galactosidase (βGal) in control and $Wnt3a^{-/-}$ mutant embryos (Fig. 2A). The *TCreERT2* line expresses a Cre recombinase-mutant estrogen receptor fusion protein in the *T* spatial domain in the PS but not in the node or notochord. For these lineage-tracing experiments TAM was injected into pregnant mothers at E7.5 and embryos were collected for analysis 24-72 h later (Fig. 2; supplementary material Fig. S2). Previous studies with *TCreERT2* at similar embryonic stages demonstrated that after a single injection of TAM, CreERT2-mediated recombination at the R26R-lacZ locus leading to the permanent expression of βGal in PS cells is evident from as early as 6-8 h post-injection, is extensive between 12 and 24 h (Anderson et al., 2013), and is likely complete

by 24 h (Nakamura et al., 2006). Thus, an injection of TAM at E7.5 largely labels a cohort of progenitors between E7.75 and E8.5. Examination of sections through the PS of E8.5 embryos for cells labeled by the *TCreERT2* transgene showed that βGal-expressing cells were found in all three germ layers and that βGal was co-expressed with the NMP marker Sox2 in most, but not all, anterior PS epithelial cells, and with the PM marker Tbx6 in the ingressed mesoderm layer (Fig. 2A). Analysis of traced E9.5 embryos similarly revealed that labeled cells contributed to neural tube, hindgut and most mesodermal descendants, with the exception of the notochord (Fig. 2B; supplementary material Fig. S2), and were maintained throughout the growing trunk region, including the progenitor zone (supplementary material Fig. S2). Taken together, these data show that the *TCreERT2* transgene labeled a *T*-expressing cell population that likely includes NMPs.

Tracing trunk progenitors in *Wnt3a*$^{-/-}$ mutants

To determine whether NMPs are the source of the cells that contribute to the ectopic neural tube in $Wnt3a^{-/-}$ mutants, T^+ PS cells were lineage traced. $Wnt3a^{-/-}$ PS cells labeled on E7.5 with *TCreERT2* and examined at E8.5 showed more labeled cells in the neural midline region of the mutant trunk than in control embryos (supplementary material Fig. S3) ($n=9$ control, $n=3$ $Wnt3a^{-/-}$ embryos). Analysis of the trunk region (s13-16) at E9.5 showed an increased proportion of labeled cells in the ectopic neural tube of $Wnt3a^{-/-}$ embryos relative to the primary neural tube (Fig. 2B,C) ($n=18$ control, $n=7$ $Wnt3a^{-/-}$ embryos). Transverse sections of three *TCreERT2*-traced wild-type embryos showed that roughly 20% of neural tube cells were labeled within the s13-16 region, whereas ~80% of PM cells were traced (Fig. 2D). In three sectioned $Wnt3a^{-/-}$ mutants, the ectopic neural tissue showed more than 60% *TCreERT2*-labeled cells, a significantly higher number than observed in the primary neural tube and comparable with the PM (Fig. 2E). These data suggest that wild-type *TCreERT2*-labeled cells differentiate into neural progenitors and PM, among others, but, in the absence of Wnt3a, cells normally fated for PM change their fate and differentiate into neural tissue. However, as the *TCreERT2* lineage also included other mesodermal and gut progenitors, a more-refined analysis was required to determine whether the ectopic neural tube in $Wnt3a^{-/-}$ mutants derived solely from the epithelial PS population.

To distinguish the $Sox2^+T^+$ epithelial PS lineage from the $Sox2^-T^+$ mesoderm and hindgut lineages (all of which are labeled with TCreERT2), we used *Cited1-CreERT2* (Boyle et al., 2008), which labels only mesodermal (and hindgut) progenitors and not the epithelial PS. Following the same protocol described above for the TCreERT2-based tracings, *Cited1-CreERT2* mice were crossed to *R26R-lacZ* and cell-tracing studies were initiated with an injection of TAM at E7.5. βGal detection was performed on E8.5-E10.5 embryos to identify *Cited1-CreERT2*-labeled cells (Fig. 2; supplementary material Fig. S2). As expected, wild-type cells labeled with *Cited1-CreERT2* were not found in the $Sox2^+$ epithelial PS at E8.5 but were detectable in mesoderm cells that had already ingressed, including $Tbx6^+$ PM (Fig. 2F; supplementary material Fig. S2). Importantly, the *Cited1-CreERT2* did not trace neural tissue; however, labeled cells were maintained throughout the extending body axis, including the posterior-most tailbud progenitor zone, days after a single pulse of TAM (Fig. 2G; supplementary material Fig. S2). This result is consistent with *Cited1-CreERT2* labeling a mesodermal progenitor population. Tracing *Cited1-CreERT2*-labeled cells in $Wnt3a^{-/-}$ mutant embryos showed a persistence of labeled cells in the trunk region at E9.5
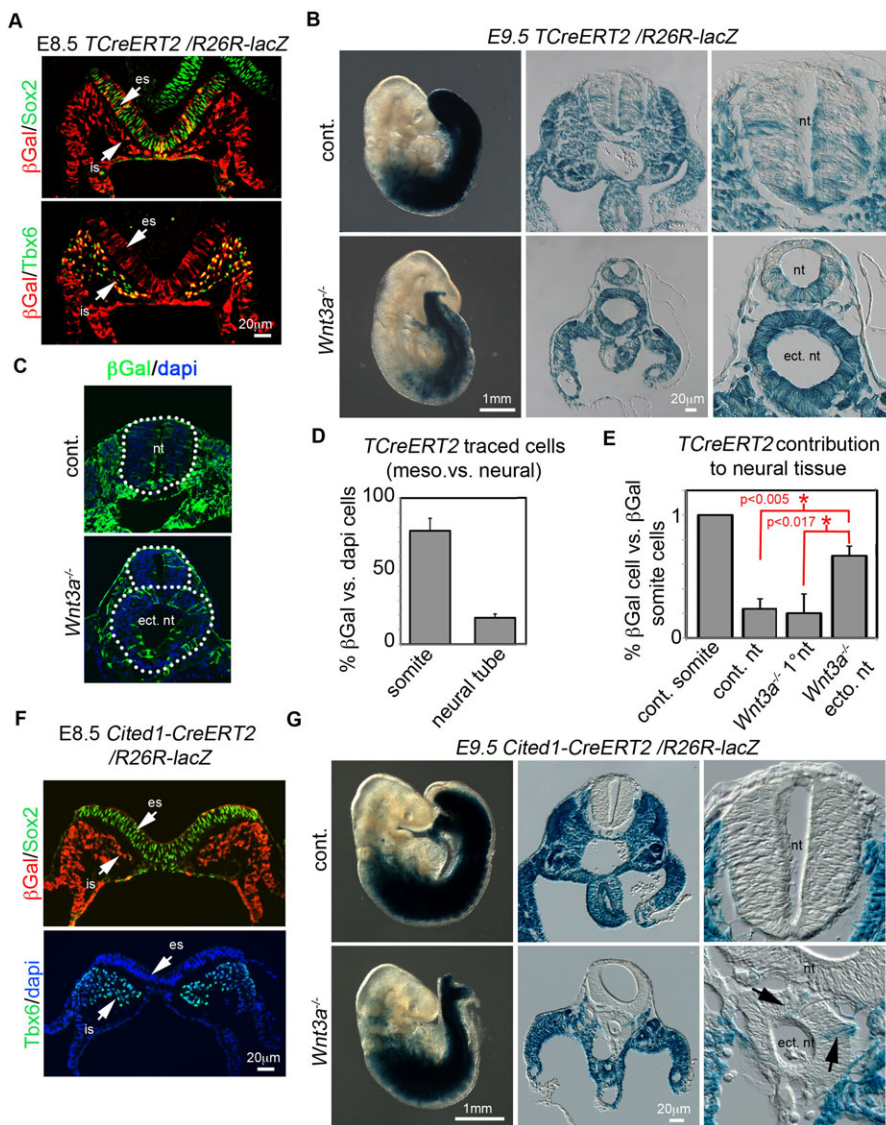
Fig. 2. Tracing trunk progenitors in *Wnt3a*^{−/−} mutants using *CreERT2;R26R-lacZ* reporters. (A) E8.5 embryo showing TCreERT2-traced βGal^{+} cells and Sox2^{+} cells (presumptive NMPs) in the epithelial PS (es), and with Tbx6^{+} cells in the ingressed PS (is). (B) βGal-stained TCreERT2 descendants (TAM administered at E7.5) in E9.5 control and *Wnt3a*^{−/−} embryos showing many βGal^{+} cells in the ectopic neural tube of *Wnt3a*^{−/−} mutants (sections through the s13-16 region). (C) Detection of βGal and DAPI to determine the number of TCreERT2-traced cells in neural and mesodermal tissues at E9.5 used in D,E. (D) Quantification of TCreERT2-labeled cells in neural versus PM tissues. Cell counts from sampled areas of three embryos. (E) Quantification of TCreERT2-labeled cells in the primary and ectopic neural tube of *Wnt3a*^{−/−} mutants (*n*=3 control, *n*=3 *Wnt3a*^{−/−}). Data are mean±s.e.m. Student's *t*-test. (F) βGal[+] Cited1-CreERT2 descendants (TAM administered at E7.5) are absent from the E8.5 epithelial PS but overlap with Tbx6^{+} ingressed streak cells. (G) βGal-stained Cited1-CreERT2 descendants (TAM at E7.5) in E9.5 control embryos show no neural contribution, and only a few traced cells in the *Wnt3a*^{−/−} ectopic neural tube (arrows). es, epithelial PS; is, ingressed PS; nt, neural tube; ect. nt, ectopic neural tube. Arrows in G indicate Cited1-CreERT2 descendants in ectopic neural tube.

(*n*=16 control, *n*=5 *Wnt3a*^{−/−} embryos). Histological analysis of *Wnt3a*^{−/−} embryos (*n*=3) showed that only a few *Cited1-CreERT2*-labeled cells were present in the ectopic neural tube of *Wnt3a*^{−/−} embryos (Fig. 2G). Typically two or three cells were observed in the ectopic neural tube per section of the mutant embryo. Considering that the ectopic neural tube contains 137.2±16.2 (s.d.) cells per section this represents roughly 2% of the ectopic neural tube cells. These data show that for cells originally destined to become mesoderm, only very few of them can change their fate, enter the neural cell lineage and contribute to the *Wnt3a*^{−/−} ectopic neural tube, after they have ingressed through the PS. The subtractive comparison between *TCreERT2* and *Cited1-CreERT2* tracings suggests that T^{+} cells (including NMPs) originating in the epithelial PS, and not the ingressed PS, primarily contribute to the ectopic neural tube.

To show that the observed change of fate from mesoderm to neural is unique to PS cells, we also examined the *Shh-Cre* traced gut and notochord lineages (Harfe et al., 2004). Examination of *Shh-Cre* traced cells in *Wnt3a*^{−/−} mutant embryos (*n*=3) showed no labeled cells occurring in the ectopic neural tube, demonstrating that NMPs do not reside in *Shh*-expressing notochord or gut progenitors (supplementary material Fig. S2).

Tracing TCreERT2-labeled cells in β-catenin loss-of-function mutants

Although Wnt3a signals through β-catenin, previous conditional deletion of *Ctnnb1* (β-catenin) in posterior progenitors with the non-inducible *T-Cre* transgenic mouse resulted in a severe loss of all trunk progenitors with no apparent ectopic neural tubes (Dunty et al., 2008). To bypass this early requirement for *Ctnnb1* and test whether NMP fate decisions are β-catenin dependent, we used the TAM-inducible *TCreERT2* transgene to conditionally delete *Ctnnb1* (*βcat*[LOF]) (Fig. 3). TAM was administered at E6.5, not at E7.5 as in previous tracing experiments, to ensure that endogenous β-catenin protein was depleted after excision of the conditional *βcat*[LOF] allele. At E9.5 the conditional *βcat*[LOF] mutants showed a malformed posterior trunk region (*n*=13/13) reminiscent of a *Wnt3a*^{−/−} mutant, with an absence of *T*-expressing trunk progenitors and defective somitogenesis (*n*=5/5) (Fig. 3A). The detection of small aggregates of somite cells can be explained by incomplete excision of β-catenin, as suggested by immunofluorescence (supplementary material Fig. S4). Histological analysis of *TCreERT2;βcat*[LOF] mutants (*n*=3) revealed enlarged and malformed neural tissue containing increased numbers of Sox2^{+} neural progenitors (Fig. 3B; supplementary material Fig. S4). Additionally, the neural tissue of *βcat*[LOF] mutants contained an
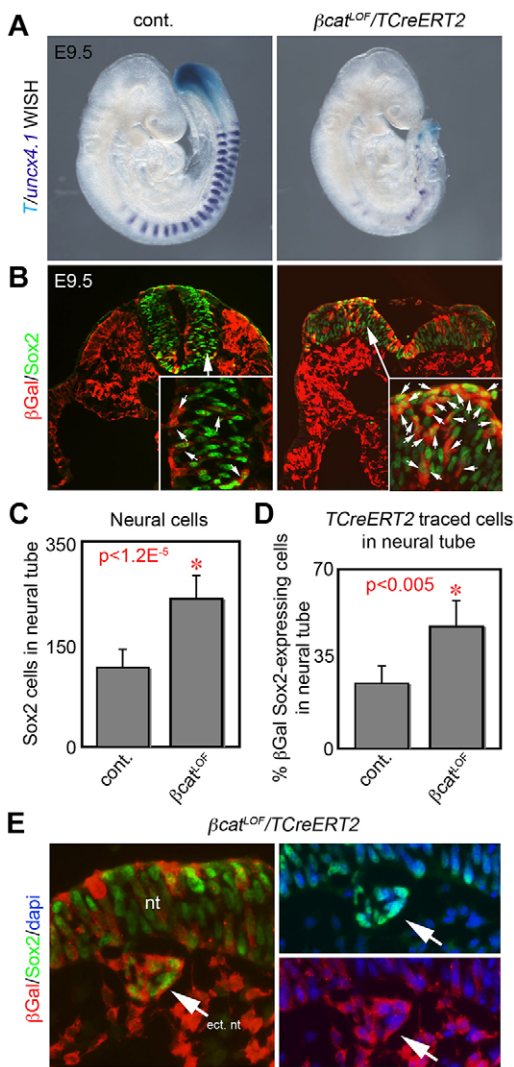
Fig. 3. TAM-regulated deletion of β-catenin ($βcat^{LOF}$) by TCreERT2.
(A) TAM-induced excision of β-catenin at E6.5 results in axial truncation at E9.5 with loss of somites (*Uncx4.1* whole-mount *in situ* hybridization, purple) and trunk progenitors (*T* whole-mount *in situ* hybridization, light blue). (B) Detection of Sox2 and βGal showing enlarged and malformed neural tube in $βcat^{LOF}$ mutant containing many TCreERT2-labeled cells (βGal). Small arrows indicate Sox2$^+$/βGal$^+$ double-positive cells. Sections taken at level equivalent to s13-16. (C) Quantification of neural cells in control (*n*=11) and $βcat^{LOF}$ (*n*=8) mutants. (D) Quantification of neural TCreERT2-labeled and Sox2$^+$ cells in control (*n*=5) and $βcat^{LOF}$ mutants (*n*=5). Data are mean±s.e.m. Student's *t*-test. (E) Analysis of Sox2 expression shows that neural progenitors found at ectopic sites in $βcat^{LOF}$ mutants are also labeled by TCreERT2 (βGal). For ease of comparison, channels are split into separate panels on the right (Sox2/ DAPI and βGal/DAPI). Arrows indicate ectopic neural structures. ect nt, ectopic neural tube; nt, neural tube.

increased proportion of *TCreERT2*-labeled cells (βGal$^+$ and Sox2$^+$). Quantification showed a doubling in neural progenitors and a doubling in the proportion of *TCreERT2*-traced cells in the neural tube, which are both indicative of a change in NM progenitor fate (Fig. 3C,D). Additionally, we observed small aggregates of ectopic neural tissue present near the embryonic midline under the primary neural tube in $βcat^{LOF}$ mutants (*n*=3) (Fig. 3E). These ectopic neural cells were *TCreERT2* traced, as evident by βGal detection, suggesting that in the absence of β-catenin signaling, T$^+$ progenitors normally destined for mesoderm will alternatively form neural cells.

β-Catenin gain-of-function is compatible with both neural and mesodermal progenitor fates

Previously it has been shown in zebrafish that activation of Wnt3a/ β-catenin signaling drives a cell to a mesodermal fate and inhibits the adoption of neural fate in a non-native niche (Martin and Kimelman, 2012), as modeled in Fig. 1A. To directly test whether Wnt signaling inhibits neural cell fate and promotes mesodermal cell fate in mammals, we increased Wnt signaling in NMPs in the native niche, using *TCreERT2* to conditionally express a dominant stabilized β-catenin (*Ctnnb1$^{lox(ex3)}$*, hereafter referred to as $βcat^{GOF}$) (Harada et al., 1999), and simultaneously trace these cells with the *R26R-lacZ* reporter. TAM was administered at E6.5 for uniformity with the $βcat^{LOF}$ studies. The resulting *TCreERT2; $βcat^{GOF}$* mutant embryos showed similar elongation of the trunk region compared with control embryos but had an irregular segmental pattern (*n*=31 controls, *n*=22 mutants). Surprisingly, section analysis of traced $βcat^{GOF}$ embryos (*n*=3) showed a similar distribution of TCreERT2; βcat^{GOF} traced cells in neural and mesodermal tissues at E10.5 to controls (*n*=3) (Fig. 4A). Examination of TCreERT2-traced cells for Sox2 expression showed that $βcat^{GOF}$ NMPs were able to enter the neural cell fate and contribute to the neural tube (Fig. 4A). Additionally, a Wnt/β-catenin reporter transgene [*BATlacZ* (Nakaya et al., 2005)] showed ectopic expression in the ventral neural tube of sectioned $βcat^{GOF}$ embryos (*n*=3) that was not observed in control embryos (*n*=3), suggesting that TCreERT2-labeled cells can differentiate into the neural lineage in the presence of elevated Wnt signaling (Fig. 4B, arrows). Only a small proportion of Wnt-responding cells were distinctively stained in the ventral neural tube, likely due to the lower Cre-excision/tracing of TCreERT2 cells in the neural tube (supplementary material Fig. S2). We also observed spheroid-shaped aggregates of Wnt reporter-responding cells throughout the trunk region of mutants (*n*=7) that were not observed in controls (*n*=8) (Fig. 4B,C). The observation that Wnt does not block entry into the neural lineage contrasts with previous reports (Martin and Kimelman, 2012; Yamaguchi et al., 1999; Yoshikawa et al., 1997); however, these data are consistent with the sustained detection of Wnt signaling in the neuroepithelium of *BATlacZ* embryos, including the epithelial PS, neuroepithelial folds and neural tube (supplementary material Fig. S5).

TCreERT2;βcat^{GOF} embryos elongate surprisingly normally up to E10.5 with no obvious truncation of the embryonic axis (Fig. 4B). Analysis of T and Sox2 in sectioned PS regions at E8.5 showed both proteins were easily detected in the PS of $βcat^{GOF}$ embryos (*n*=3) (Fig. 4D). However, the morphology of the $βcat^{GOF}$ PS was abnormal with a broader and thinner epithelium (Fig. 4D). $βcat^{GOF}$ embryos also showed increased expression of T, consistent with the known role of *T* as a transcriptional target of Wnt/β-catenin signaling (Yamaguchi et al., 1999). Combined, these data are consistent with Wnt signals maintaining multipotent NMPs *in vivo*, as recently demonstrated *in vitro* (Tsakiridis et al., 2014).

Notably, the most prominent phenotype of constitutive Wnt/β-catenin signaling in the trunk region of the *TCreERT2;βcat^{GOF}* embryos was the formation of aggregates of undifferentiated progenitors along the length of the embryo (Fig. 4C). These aggregates were similar histologically to PS progenitors and, like PS tissue, highly responsive to Wnt signaling (Fig. 4C). To determine which progenitors were being promoted by Wnt/β-catenin signaling, markers of NMPs (Sox2$^+$T$^+$), PMPs (Tbx6$^+$T$^+$) and presomitic mesoderm (Tbx6$^+$T$^-$) were used in immunofluorescent studies of sectioned βcat^{GOF} embryos (*n*=3) (Fig. 5A). This analysis suggests that Wnt signaling promotes both mesodermal progenitors
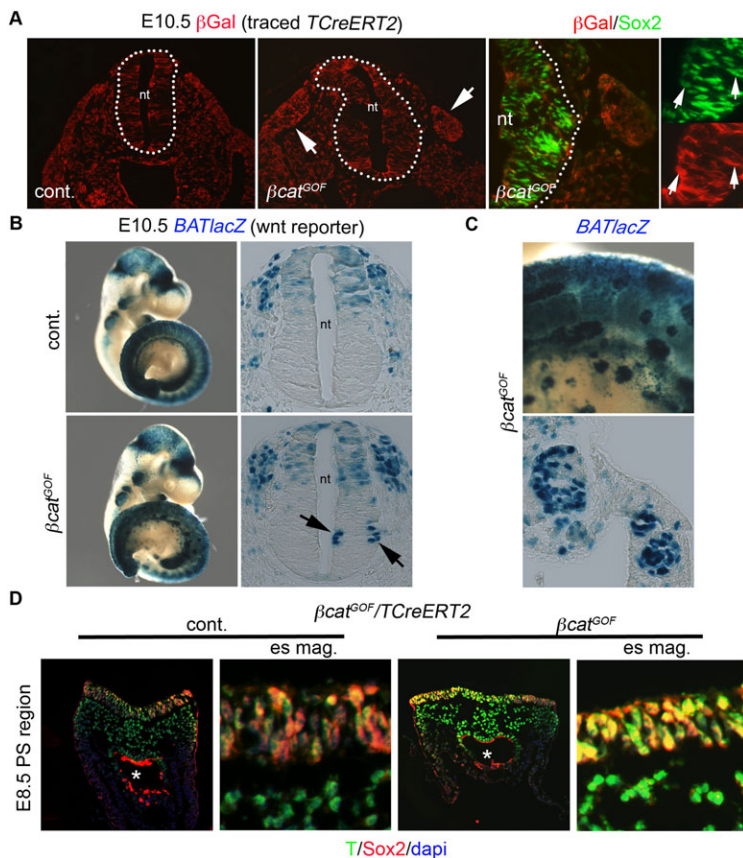
DEVELOPMENT

Fig. 4. Elevated β-catenin activity (βcat^{GOF}) in TCreERT2-expressing progenitors does not inhibit neural progenitor formation or NMP formation in the epithelial PS. (A) Lineage-traced TCreERT2 descendants (TAM administered at E6.5) (βGal$^+$) that are also expressing a dominant-active β-catenin (βcat^{GOF}) aggregate in the trunk of the E10.5 embryo (arrows). Co-detection of βGal and Sox2 (arrows, right panel) show that TCreERT2-traced βcat^{GOF} cells in the neural tube are neural progenitors. (B) Whole-mount βGal staining to detect BATlacZ (Wnt/β-catenin reporter) activity in control and βcat^{GOF} embryos show ectopic clumps of active Wnt signaling cells. Cross-section of the neural tube region (right panels) shows ectopic Wnt activity in the ventral neural tube of βcat^{GOF} embryos (arrows). (C) Magnified views of BATlacZ activity in βcat^{GOF} embryo showing clumps of βgal-expressing cells in whole mount (top) and in a cross-section (bottom) through trunk mesoderm. (D) Detection of NMP markers T and Sox2 in the PS region of control and βcat^{GOF} embryos. Magnified views of the epithelial PS (es mag). Asterisks indicate non-Sox2 secondary detection in the gut lumen. nt, neural tube.

and presomitic mesoderm types. We did not observe Sox2$^+$T$^+$ co-expressing cells in aggregates, indicating that Wnt signaling, or at least prolonged Wnt signaling, maintained TCreERT2-labeled progenitors in a mesodermal state (Fig. 5A).

To distinguish whether Wnt-induced mesodermal progenitor maintenance occurred specifically in NMPs or in mesodermal progenitors, we took advantage of the *Cited1-CreERT2* transgene (Fig. 2F). *Cited1-CreERT2;βcat^{GOF}* embryos (TAM administered at E6.5) elongated similarly to controls but had abnormal trunk morphology at E10.5 (*n*=11 control, *n*=9 mutants). Sections of *Cited1-CreERT2;βcat^{GOF}* embryos (*n*=3) showed that the constitutive activation of β-catenin in mesoderm led to the formation of irregularly shaped aggregates of PMPs (Tbx6$^+$T$^+$) and presomitic mesoderm (Tbx6$^+$T$^-$), but not Sox2$^+$T$^+$ NMPs (Fig. 5B). This phenotype is very similar to that observed when β-catenin is expressed in T+ progenitors (via *TCreERT2*) (Fig. 5A), suggesting that the maintenance of mesodermal progenitor fate by Wnt signaling occurs in already-specified mesodermal progenitors.

Implicit in the βcat^{GOF} studies above is that Wnt functions to maintain progenitors. To test this hypothesis, we traced the progeny of permanently labeled *TCreERT2;βcat^{GOF}* cells (TAM administered at E6.5) using *R26R-lacZ* to determine whether they differentiated into neurons or PM derivatives such as myocytes (Fig. 6). This analysis showed that traced βcat^{GOF} cells were disproportionately associated with Sox2$^+$ neuronal progenitors in the ventricular zone in the medial neural tube, whereas control traced cells were widely distributed throughout the neural tube (*n*=4 control, *n*=4 mutants) (Fig. 6A). Quantification showed that traced βcat^{GOF} cells were twice as likely as control cells to be associated with Sox2$^+$ progenitor populations (Fig. 6B). During

development, Sox2-expressing neural progenitors do not express neural differentiation markers (Graham et al., 2003). Analysis of the expression of Sox2 and the neuronal differentiation marker neurofilament indeed showed that these βcat^{GOF}-expressing Sox2$^+$ progenitors were undifferentiated (Fig. 6C). Similarly, we used skeletal muscle myosin (MF20), a terminal myocyte marker, to determine whether *TCreERT2;βcat^{GOF}* cells become myocytes (Fig. 6D). This was assessed in E9.5 embryos (injected with TAM at E7.5) by examining whether βGal$^+$;βcat^{GOF} cells entered the MF20 lineage. In control embryos, traced *TCreERT2* cells were frequently observed entering a MF20$^+$ myocyte fate; however, βcat^{GOF} cells were much less likely to do so (Fig. 6E). These data suggest that persistent Wnt signaling in *TCreERT2*-traced progenitors inhibits their differentiation.

Loss of NMPs in *Wnt3a$^{-/-}$* embryos

To determine the fate of NMPs in *Wnt3a$^{-/-}$* mutants, we examined E8.5 embryos for the presence of Sox2- and T-expressing populations. In *Wnt3a$^{-/-}$* embryos (*n*=3), Sox2 and T colocalization was not detected in the anterior PS: Sox2 was readily detected; however, T was not (Fig. 7A). For embryo-wide perspective of *Sox2* and *T* co-expression, we employed whole-mount *in situ* hybridization detection. Two-color whole-mount *in situ* hybridization showed that *Sox2* and *T* transcripts were co-expressed in control anterior PS regions at E8.5 (*n*=8). In *Wnt3a$^{-/-}$* embryos, the *Sox2*-expressing zone was expanded posteriorly while the *T* expressing domain was dramatically reduced to the posterior most tip of the PS (*n*=3) (Fig. 7B). This loss of *Sox2* and *T* co-expressing zones is consistent with *in vitro* studies where Sox2$^+$ progenitors, but not Sox2$^+$T$^+$ progenitors, form in the absence of Wnt signaling in differentiating epiblast progenitors (Tsakiridis et al., 2014). It is, however, unknown
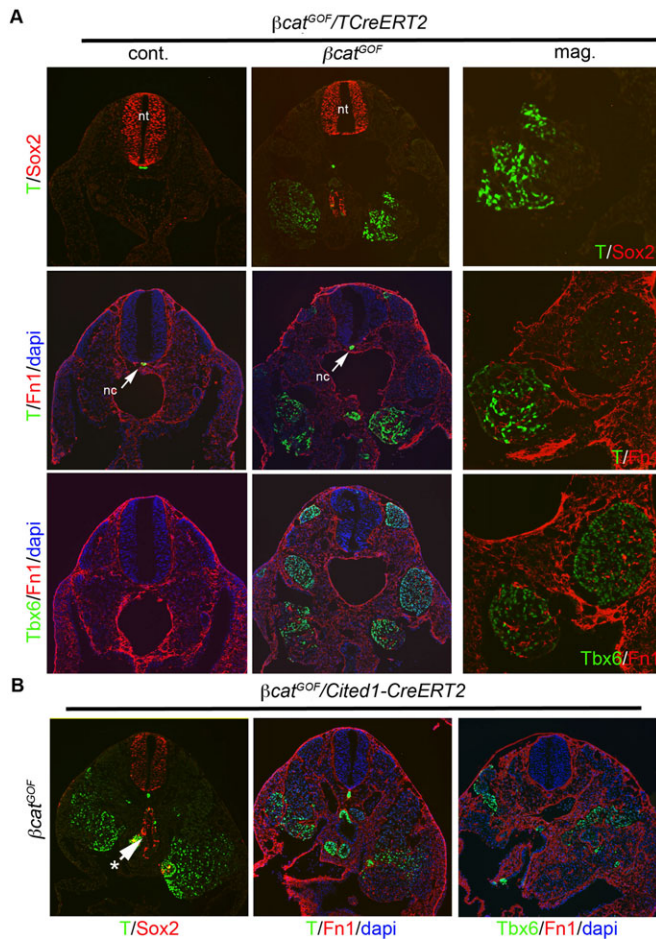
Fig. 5. Elevated β-catenin signaling (βcat^{GOF}) maintains mesodermal progenitors. (A) Detection of NMP markers (T^+Sox2^+), PMPs ($Tbx6^+T^+$) and presomitic mesoderm ($Tbx6^+T^-$) in $TCreERT2$ βcat^{GOF} and control embryos at E10.5 (TAM treatment at E6.5). Magnified regions on the right show the expression of T and Tbx6 in adjacent sections of the same embryo. nc, neural crest; nt, neural tube. (B) Detection of markers in $Cited1$-$CreERT2$ βcat^{GOF} embryos at E10.5 in which β-catenin is elevated and maintained only in ingressed PS cells (TAM treatment at 6.5). Asterisk with arrow indicates non-Sox2 secondary detection in the gut lumen.

what happens to the NMP population in the absence of Wnt signaling.

To test whether NMPs were being lost by cell death, we examined the PS of control ($n=3$) and $Wnt3a^{-/-}$ ($n=3$) embryos for apoptotic cells using an antibody to cleaved caspase 3. It has been previously shown that apoptosis occurs in the $Wnt3a$ hypomorphic mutant, *vestigial tail* (*vt*), within the caudal axis (Shum et al., 1999). In $Wnt3a^{-/-}$ mutant embryos, cleaved caspase 3 was readily detected in cells of the epithelial PS, with some dying cells in the ingressed PS (Fig. 6C). Dying cells were observed along the lateral length of the mutant PS at E8.5 by whole-mount detection with LysoTracker Red ($n=7$) (supplementary material Fig. S6) (Fogel et al., 2012). To further explore whether NMPs were being lost in $Wnt3a^{-/-}$ mutants, we attempted to label this PS population with $TCreERT2$, while cell death was occurring, by injecting TAM at E8.0 (rather than at E7.5, as described above). Examination of control embryos at E9.75 showed many labeled trunk progenitor cells similar to lineage-tracing experiments when TAM is injected at E7.5 ($n=14$); however, $Wnt3a^{-/-}$ embryos showed very few labeled cells ($n=6$) (Fig. 6D). These data indicate

that either $TCreERT2$-traced cells are being lost in $Wnt3a^{-/-}$ embryos or, alternatively, that T expression is being lost. However, loss of T itself may be crucial for NMP survival, and thus synonymous with a loss of NMP fate. Together, these data support a model in which Wnt3a is required to maintain the NMP.

DISCUSSION

Using transgenic approaches, we traced the behavior of T-expressing posterior progenitor populations to understand how NMP cell fate decisions are controlled by Wnt/β-catenin signaling *in vivo*. We find that Wnt/β-catenin signals are necessary for the survival of $Sox2^+T^+$ NMPs and their descendants ($Tbx6^+T^+$ PMPs and $Tbx6^+T^-$ PSM), and that constitutive expression of Wnt/β-catenin signals in NMPs and their descendants locks cells in a progenitor state. These studies suggest that Wnts act as progenitor growth factors, and that differentiation and exit from the progenitor state requires a reduction in Wnt signaling. This activity is consistent with that described for Wnts in the self-renewal of stem cells in multiple adult tissues (reviewed by Clevers and Nusse, 2012).

It has been previously proposed that high Wnt signaling suppresses neural progenitor development, as inhibition of the Wnt pathway results in ectopic neural tissue (Kondoh and Takemoto, 2012; Martin and Kimelman, 2012; Takada et al., 1994). However, this interpretation is unlikely as our genetic gain-of-function data suggest that neural progenitors can form in the presence of high Wnt signaling *in vivo*. Recent modeling of stem cell differentiation *in vitro* also shows that Wnt signaling can enhance neural progenitor formation (Turner et al., 2014). Indeed, positive Wnt-responsive elements have been identified within the *Sox2 N1* enhancer that drives *Sox2* expression in neural progenitors (Takemoto et al., 2011). Furthermore, Wnt/β-catenin reporter expression in the developing trunk showed that high Wnt activity in epithelial PS cells continues through more anteriorly localized neural progenitors (Ferrer-Vaquer et al., 2010). Combined, these data suggest that Wnt activity is compatible with the self-renewal of both neural and mesodermal progenitors. Considering that the expression of T in the hindgut endoderm also depends upon Wnt3a, we suggest that Wnts promote posterior development by maintaining progenitors in all three germ layers.

Our use of TAM-inducible Cre transgenic lines, in concert with the $R26R$-$lacZ$ reporter, allowed for a germ layer-specific characterization of cell lineages arising in the PS. The $TCreERT2$ transgene permitted the permanent, temporally restricted tracing of T-expressing cell lineages across all three germ layers, including the neuroepithelium and the epithelial layer of the PS. $TCreERT2$ and $Cited1$-$CreERT2$ traced similar mesodermal and endodermal populations; however, $Cited1$-$CreERT2$ did not label the epithelial streak or neural tube. Thus, $TCreERT2$ uniquely labeled the neuroepithelium and PS epithelium. By subtracting the $Cited1$-$CreERT2$ labeled cells from the $TCreERT2$ population in wild-type and $Wnt3a^{-/-}$ embryos, we were able to deduce that cells capable of giving rise to both neural and paraxial mesoderm primarily reside in the epithelial PS. This result is consistent with $TCreERT2$ labeling a population of epithelial PS cells that include NMPs. As some $Cited1$-$CreERT2$-labeled $Wnt3a^{-/-}$ cells also contribute to the ectopic neural tube it suggests that some already-ingressed 'mesodermal' PS cells retain NMP potential, consistent with $Sox2^+T^+$ co-expression in cells of the ingressed PS. Additionally, we used *Shh-Cre*-based tracings to exclude notochord and endoderm as sources of cells with NMP potential. Thus, lineage tracing and Sox2/T marker analysis arrive at similar conclusions regarding the location of NMPs in the epithelial PS. It remains
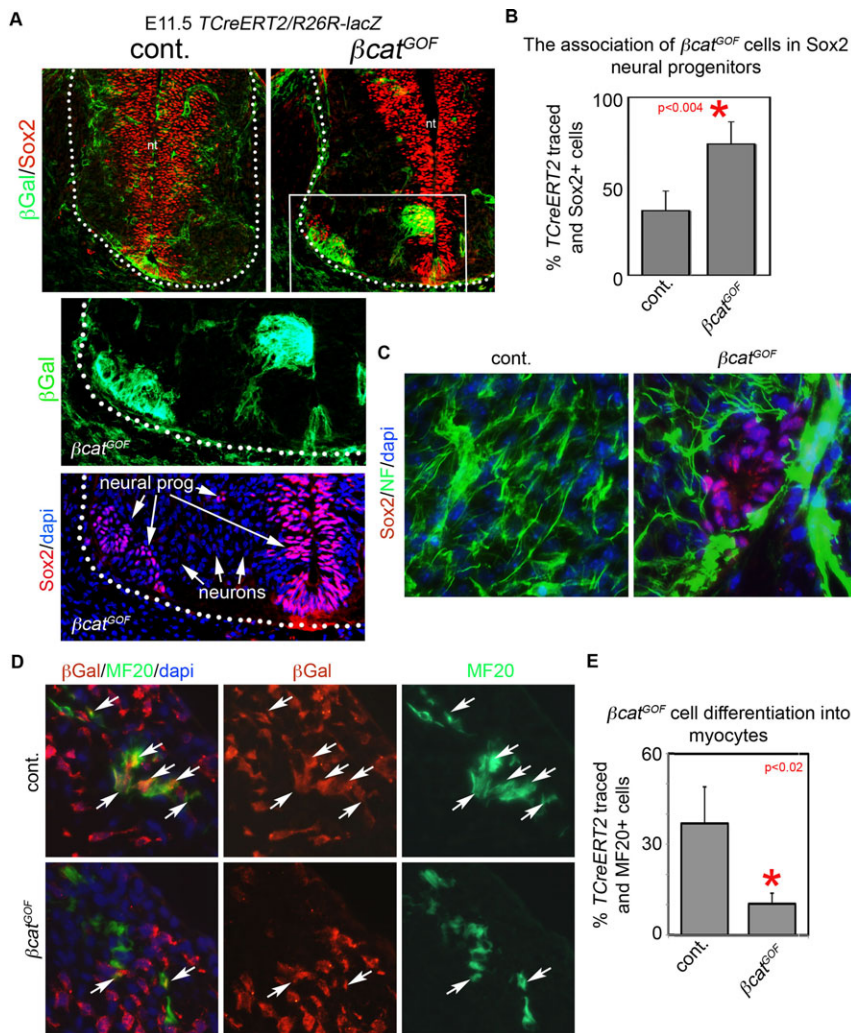
Fig. 6. TCreERT2-traced cells with elevated β-catenin activity do not readily contribute to differentiated neurons or myocytes. (A) Detection of Sox2 (neural progenitors) at E11.5 in the medial ventricular region of the neural tube with control *TCreERT2*-traced cells (βGal) or *βcat^{GOF};TCreERT2*-traced cells (βGal) (TAM treatment at E6.5). nt, neural tube. (B) Quantitation of *TCreERT2*-traced cells colocalized with Sox2 in the neural tube from control (*n*=4) and *βcat^{GOF}* (*n*=4) stage-matched embryos. Data are mean±s.e.m. *P*<0.004, Student's *t*-test. (C) Detection of Sox2 (neural progenitors) and neurofilament protein (neurons) in the lateral region of the neural tube in control and *βcat^{GOF};TCreERT2* embryos. (D) Detection of MF20 (myocytes) at E9.5 in an anterior somite in *TCreERT2*-traced cells (βGal) and *βcat^{GOF}; TCreERT2*-traced cells (βGal) (TAM treatment at E7.5). Arrows mark βGal$^+$/MF20$^+$ cells. (E) Quantitation of *TCreERT2*-traced cells (βGal$^+$) and MF20-expressing myocytes in control (*n*=4) and *βcat^{GOF}* (*n*=4) stage-matched embryos. Total number of MF20$^+$ cells in the sampled region is not significantly different between control and *βcat^{GOF}* embryos, but the number of double-positive cells is. Data are mean±s.e.m. *P*<0.02, Student's *t*-test.

formally possible that self-renewing progenitors with neural-restricted potential are also labeled in the *TCreERT2* lineage analysis; however, we are unable to address this possibility with the currently available Cre drivers.

Previous studies have shown that axial progenitors display unique behavior in that they can be serially transplanted back into hosts of a younger developmental age and continue to contribute to the developing axis (Cambray and Wilson, 2002; Tam and Tan, 1992). Detailed retrospective clonal lineage analyses provide further evidence for a persistent pool of bipotent self-renewing NMPs (Wilson et al., 2009). Our data demonstrating that a single dose of TAM in *TCreERT2* mice labeled NMPs that remained in the epithelial PS or tailbud for at least 3 days of development suggest that these posterior progenitors have self-renewing characteristics and are consistent with the concept that NMPs could be a stem cell population; however, a convincing demonstration that NMPs are long-term self-renewing stem cells remains to be shown.

Tracing the fate of PS cells in the *Wnt3a$^{-/-}$* mutant background was essential to localize NMPs functionally, and to validate Sox2 and T co-expression as markers of NMPs within the PS. Based on Sox2/T co-expression at E8.5, the majority of the anterior epithelial PS cells are NMPs at this stage; however, we have not proven that all Sox2$^+$T$^+$ cells have the capacity to self-renew. Previous labeling experiments near this region show that it gives rise mainly to PM, while more posterior PS regions give rise to lateral and extra-embryonic mesoderm (Tam and Beddington, 1987). As PM is derived from the anterior PS, and nearly all anterior PS cells express Sox2 and T, it follows that the majority of trunk PM is derived from NMPs. Furthermore, a substantial proportion of the neural cells of the posterior trunk are derived from a *T*-expressing lineage. Taken together, NMPs likely produce the vast majority of neural and PM-derived tissue of the posterior axis. Given that the *TCreERT2* mouse line was created through standard transgene insertion methods, it remains formally possible that the *TCreERT2* transgene could label Sox2$^+$T$^-$ neural progenitors (i.e. cells outside of the normal *T* expression domain), which would lead to an overestimate of the neural contribution of NMPs. Alternatively, progenitor populations would be underestimated if the TCreERT2 transgene does not label all Sox2$^+$T$^+$ NMPs. Regardless, our data show that Wnt-dependent multipotent progenitors play an essential role in the formation of the posterior axis of developing mammalian embryos and further underscore the crucial role that T plays in cell fate determination.
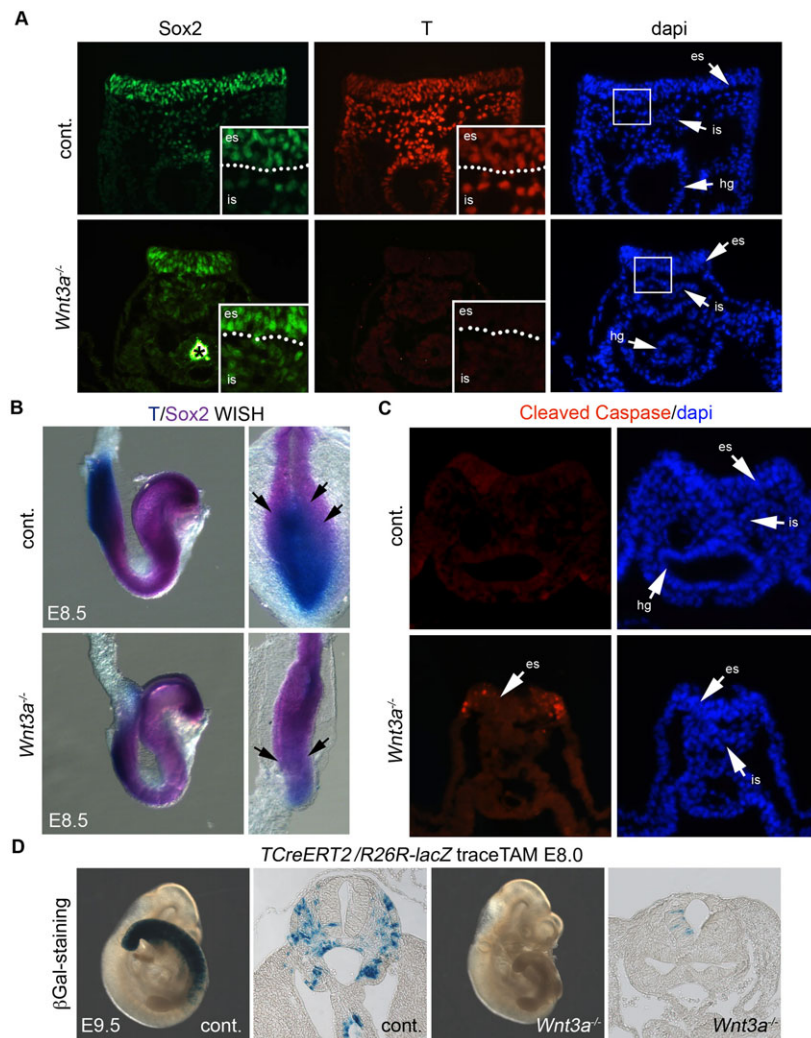
MATERIALS AND METHODS
Animals

Fig. 7. Localization of NMPs in the PS region and their resultant fate in *Wnt3a*⁻/⁻ mutants. (A) Detection of Sox2 and T in the anterior PS at E8.5 in epithelialized PS (es) and ingressed PS (is). *Wnt3a*⁻/⁻ embryos show Sox2, but not T, expression in both epithelial and ingressed PS populations. Asterisk indicates non-specific secondary antibody detection in the hindgut (hg). (B) Whole-mount *in situ* hybridization of *Sox2* and *T* expression in the PS region of E8.5 control and *Wnt3a*⁻/⁻ mutants. Arrows indicate transition zone of *T/Sox2* expression. (C) Detection of cleaved caspase 3 in sections through the mid PS region at E8.5. (D) βGal staining of *TCreERT2*-traced cells in E9.75 control and *Wnt3a*⁻/⁻ mutants exposed to TAM at E8.0. es, epithelial PS; is, ingressed PS.

TCreERT2 or *Cited1-CreERT2*-expressing progenitors in control and *Wnt3a*⁻/⁻ mutants was initiated by injection of pregnant mothers with TAM at E7.5 as described previously (Anderson et al., 2013). Any reduction of TAM dose resulted in a reduction in labeled cells, indicating that TAM was not in excess. $\beta cat^{LOF};TCreERT2$ and $\beta cat^{GOF};TCreERT2$ cell lineage studies were initiated with TAM administered at E6.5. For determination of Wnt activation, the βcat^{GOF} line was bred with *BATlacZ* (Nakaya et al., 2005). This study was carried out in compliance with the Guide for the Care and Use of Laboratory Animals of the National Institutes of Health (Frederick National Lab Animal Care and Use Committee Proposal #12-408). Rodents were euthanized by CO_2 inhalation in accordance with the most recent AVMA Guidelines on Euthanasia.

Histology and immunohistochemistry

Antibody detection in frozen section was performed as previously described (Dunty et al., 2014) using primary antibodies to Sox2 (R&D Systems, mab2018, 1:100; Millipore, AB5603, 1:100-1:1000); T (R&D Systems, AF2085, 1:100), fibronectin (DakoCytomation, A0245, 1:500); MF20 (DSHB,1:20); neurofilament protein (DSHB 2H3-c,1:100); Tbx6 (R&D Systems, AF4744, 1:100), Pax7 (DSHB, 1:20), Sox9 (Millipore, Ab5535, 1:100), β-galactosidase (MP Biomedicals, 559761, 1:5000) and β-catenin (BD Bioscience, 610154, 1:400). For paraffin sectioning, embryos were dehydrated in ethanol, cleared in citrisolv (Fisher) for 2×20 min, embedded in 3×20 min changes of molten paraffin (Fisher) and then sectioned at 5 µm. Detection of p-Histone H3 (Cell Signaling, #97065, 1:200) and cleaved caspase 3 (Millipore, AB3623, 1:200) was performed on dewaxed/rehydrated slides boiled in 10 mM sodium citrate (pH 6) for 20 min

followed by immunohistochemistry procedures used on frozen section. Alcian Blue 8GX (Sigma) was used to make a 1% staining solution in 3% acetic acid (final pH 2.5). Rehydrated paraffin sections were stained for 1 h, rinsed in tap water and then PBS, counterstained in nuclear Fast Red solution (0.1% NFR, 5% aluminum sulfate), and rinsed in PBS before ethanol dehydration and mounting with permount (Fisher).

In situ hybridization and βGal staining

Whole-mount *in situ* hybridization was performed using a modification (Biris et al., 2007) of previously described methods (Harland, 1991) with antisense RNA probes using digoxigenin- or fluorescein-labeled UTP (Roche) for synthesis of *Sox2*, *T* and *Uncx4.1* RNA probes (Invitrogen). For color development, NBT/BCIP (dark purple, Roche), BCIP alone (light blue) or magenta phosphate (magenta, Goldbio) were used as substrates. Whole-mount βGal staining was performed as described previously (Ahn et al., 2013; Whiting et al., 1991). For lineage-tracing studies, labeled cells were identified by direct detection of βGal with specific antibodies (Fig. 2A) or through the enzymatic activity of βGal (Fig. 2B, supplementary material Fig. S2). LysoTracker Red was used as previously described (Fogel et al., 2012).

Imaging, quantification and analysis

Acquired digital images were prepared in Photoshop with adjustments to color, magnification, brightness and contrast applied equally to images under comparison. Cell counts for proliferation rates and *Cited1-CreERT2; Wnt3a*⁻/⁻ lineage studies represented the total cell count from tissues analyzed averaged over five consecutive sections per embryo. Sibling

embryos of similar size were compared in analysis containing $Wnt3a^{-/-}$ and $TCreERT2;\beta cat^{LOF}$ mutants, as they lack a full complement of somites typically used to accurately stage match embryos. Variation in overall embryo proliferation rates was observed among sibling embryos regardless of genotype. To better compare embryos, we normalized the neural proliferation rate by dividing this rate with the proliferation rate of non-PM (intermediate and lateral plate mesoderm), as this tissue forms normally in $Wnt3a^{-/-}$ mutants. The resulting calculation produces a ratio used for comparisons of proliferation rate. For comparisons of lineage and cell fate, the quantifications are derived from sampled representative regions of 30 cells or more using DAPI-stained nuclei as a counting standard. Comparisons of lineage-traced cell fate were presented as a percent from each sampled embryo, and multiple samples were used to calculate average, standard deviations and t-test (two-tailed) statistical comparisons.

Supplementary material
Supplementary material available online at
http://dev.biologists.org/lookup/suppl/doi:10.1242/dev.111922/-/DC1

References
Ahn, Y., Sims, C., Logue, J. M., Weatherbee, S. D. and Krumlauf, R. (2013). Lrp4 and Wise interplay controls the formation and patterning of mammary and other skin appendage placodes by modulating Wnt signaling. *Development* **140**, 583-593.

Anderson, M. J., Naiche, L. A., Wilson, C.P., Elder, C., Swing, D. A. and Lewandoski, M. (2013). TCreERT2, a transgenic mouse line for temporal control of Cre-mediated recombination in lineages emerging from the primitive streak or tail bud. *PLoS ONE* **8**, e62479.

Bellairs, R. (1986). The primitive streak. *Anat. Embryol.* **174**, 1-14.

Biris, K. K., Dunty, W. C., Jr and Yamaguchi, T. P. (2007). Mouse Ripply2 is downstream of Wnt3a and is dynamically expressed during somitogenesis. *Dev. Dyn.* **236**, 3167-3172.

Boyle, S., Misfeldt, A., Chandler, K. J., Deal, K. K., Southard-Smith, E. M., Mortlock, D. P., Baldwin, H. S. and de Caestecker, M. (2008). Fate mapping using Cited1-CreERT2 mice demonstrates that the cap mesenchyme contains self-renewing progenitor cells and gives rise exclusively to nephronic epithelia. *Dev. Biol.* **313**, 234-245.

Brault, V., Moore, R., Kutsch, S., Ishibashi, M., Rowitch, D. H., McMahon, A. P., Sommer, L., Boussadia, O. and Kemler, R. (2001). Inactivation of the beta-catenin gene by Wnt1-Cre-mediated deletion results in dramatic brain malformation and failure of craniofacial development. *Development* **128**, 1253-1264.

Cambray, N. and Wilson, V. (2002). Axial progenitors with extensive potency are localised to the mouse chordoneural hinge. *Development* **129**, 4855-4866.

Cambray, N. and Wilson, V. (2007). Two distinct sources for a population of maturing axial progenitors. *Development* **134**, 2829-2840.

Clevers, H. and Nusse, R. (2012). Wnt/beta-catenin signaling and disease. *Cell* **149**, 1192-1205.

Dunty, W. C., Jr, Biris, K. K., Chalamalasetty, R. B., Taketo, M. M., Lewandoski, M. and Yamaguchi, T. P. (2008). Wnt3a/beta-catenin signaling controls posterior body development by coordinating mesoderm formation and segmentation. *Development* **135**, 85-94.

Dunty, W. C., Jr, Kennedy, M. W. L., Chalamalasetty, R. B., Campbell, K. and Yamaguchi, T. P. (2014). Transcriptional profiling of Wnt3a mutants identifies Sp

transcription factors as essential effectors of the Wnt/beta-catenin pathway in neuromesodermal stem cells. *PLoS ONE* **9**, e87018.

Ferrer-Vaquer, A., Piliszek, A., Tian, G., Aho, R. J., Dufort, D. and Hadjantonakis, A.-K. (2010). A sensitive and bright single-cell resolution live imaging reporter of Wnt/ss-catenin signaling in the mouse. *BMC Dev. Biol.* **10**, 121.

Fogel, J. L., Thein, T. Z. T. and Mariani, F. V. (2012). Use of LysoTracker to detect programmed cell death in embryos and differentiating embryonic stem cells. *J. Vis. Exp.* **68**, e4254.

Galceran, J., Farinas, I., Depew, M. J., Clevers, H. and Grosschedl, R. (1999). Wnt3a-/–like phenotype and limb deficiency in Lef1(-/-)Tcf1(-/-) mice. *Genes Dev.* **13**, 709-717.

Garcia-Martinez, V. and Schoenwolf, G. C. (1992). Positional control of mesoderm movement and fate during avian gastrulation and neurulation. *Dev. Dyn.* **193**, 249-256.

Göthert, J. R., Gustin, S. E., Hall, M. A., Green, A. R., Göttgens, B., Izon, D. J. and Begley, C. G. (2005). In vivo fate-tracing studies using the Scl stem cell enhancer: embryonic hematopoietic stem cells significantly contribute to adult hematopoiesis. *Blood* **105**, 2724-2732.

Graham, V., Khudyakov, J., Ellis, P. and Pevny, L. (2003). SOX2 functions to maintain neural progenitor identity. *Neuron* **39**, 749-765.

Harada, N., Tamai, Y., Ishikawa, T.-o., Sauer, B., Takaku, K., Oshima, M. and Taketo, M. M. (1999). Intestinal polyposis in mice with a dominant stable mutation of the beta-catenin gene. *EMBO J.* **18**, 5931-5942.

Harfe, B. D., Scherz, P. J., Nissim, S., Tian, H., McMahon, A. P. and Tabin, C. J. (2004). Evidence for an expansion-based temporal Shh gradient in specifying vertebrate digit identities. *Cell* **118**, 517-528.

Harland, R. M. (1991). In situ hybridization: an improved whole-mount method for Xenopus embryos. *Methods Cell Biol.* **36**, 685-695.

Herrmann, B. G. (1992). Action of the Brachyury gene in mouse embryogenesis. *Ciba Found. Symp.* **165**, 78-86; discussion 86-91.

Kondoh, H. and Takemoto, T. (2012). Axial stem cells deriving both posterior neural and mesodermal tissues during gastrulation. *Curr. Opin. Genet. Dev.* **22**, 374-380.

Li, R. A. and Storey, K. G. (2011). An emerging molecular mechanism for the neural vs mesodermal cell fate decision. *Cell. Res.* **21**, 708-710.

Martin, B. L. and Kimelman, D. (2008). Regulation of canonical Wnt signaling by Brachyury is essential for posterior mesoderm formation. *Dev. Cell* **15**, 121-133.

Martin, B. L. and Kimelman, D. (2012). Canonical Wnt signaling dynamically controls multiple stem cell fate decisions during vertebrate body formation. *Dev. Cell* **22**, 223-232.

Masahira, N., Takebayashi, H., Ono, K., Watanabe, K., Ding, L., Furusho, M., Ogawa, Y., Nabeshima, Y.-c., Alvarez-Buylla, A., Shimizu, K. et al. (2006). Olig2-positive progenitors in the embryonic spinal cord give rise not only to motoneurons and oligodendrocytes, but also to a subset of astrocytes and ependymal cells. *Dev. Biol.* **293**, 358-369.

Nakamura, E., Nguyen, M.-T. and Mackem, S. (2006). Kinetics of tamoxifen-regulated Cre activity in mice using a cartilage-specific CreER(T) to assay temporal activity windows along the proximodistal limb skeleton. *Dev. Dyn.* **235**, 2603-2612.

Nakaya, M.-a., Biris, K., Tsukiyama, T., Jaime, S., Rawls, J. A. and Yamaguchi, T. P. (2005). Wnt3alinks left-right determination with segmentation and anteroposterior axis elongation. *Development* **132**, 5425-5436.

Schepers, A. G., Snippert, H. J., Stange, D. E., van den Born, M., van Es, J. H., van de Wetering, M. and Clevers, H. (2012). Lineage tracing reveals Lgr5+ stem cell activity in mouse intestinal adenomas. *Science* **337**, 730-735.

Schoenwolf, G. C., Garcia-Martinez, V. and Dias, M. S. (1992). Mesoderm movement and fate during avian gastrulation and neurulation. *Dev. Dyn.* **193**, 235-248.

Shum, A. S. W., Poon, L. L. M., Tang, W. W. T., Koide, T., Chan, B. W. H., Leung, Y.-C. G., Shiroishi, T. and Copp, A. J. (1999). Retinoic acid induces down-regulation of Wnt-3a, apoptosis and diversion of tail bud cells to a neural fate in the mouse embryo. *Mech. Dev.* **84**, 17-30.

Soriano, P. (1999). Generalized lacZ expression with the ROSA26 Cre reporter strain. *Nat. Genet.* **21**, 70-71.

Srinivasan, R. S., Dillard, M. E., Lagutin, O. V., Lin, F.-J., Tsai, S., Tsai, M.-J., Samokhvalov, I. M. and Oliver, G. (2007). Lineage tracing demonstrates the venous origin of the mammalian lymphatic vasculature. *Genes Dev.* **21**, 2422-2432.

Takada, S., Stark, K. L., Shea, M. J., Vassileva, G., McMahon, J. A. and McMahon, A. P. (1994). Wnt-3a regulates somite and tailbud formation in the mouse embryo. *Genes Dev.* **8**, 174-189.

Takemoto, T., Uchikawa, M., Yoshida, M., Bell, D. M., Lovell-Badge, R., Papaioannou, V. E. and Kondoh, H. (2011). Tbx6-dependent Sox2 regulation determines neural or mesodermal fate in axial stem cells. *Nature* **470**, 394-398.

Tam, P. P. and Beddington, R. S. (1987). The formation of mesodermal tissues in the mouse embryo during gastrulation and early organogenesis. *Development* **99**, 109-126.

Tam, P. P. L. and Behringer, R. R. (1997). Mouse gastrulation: the formation of a mammalian body plan. *Mech. Dev.* **68**, 3-25.

Tam, P. P. and Tan, S. S. (1992). The somitogenetic potential of cells in the primitive streak and the tail bud of the organogenesis-stage mouse embryo. *Development* **115**, 703-715.

Tsakiridis, A., Huang, Y., Blin, G., Skylaki, S., Wymeersch, F., Osorno, R., Economou, C., Karagianni, E., Zhao, S., Lowell, S. et al. (2014). Distinct Wnt-driven primitive streak-like populations reflect in vivo lineage precursors. *Development* **141**, 1209-1221.

Turner, D. A., Hayward, P. C., Baillie-Johnson, P., Rue, P., Broome, R., Faunes, F. and Martinez Arias, A. (2014). Wnt/beta-catenin and FGF signalling direct the specification and maintenance of a neuromesodermal axial progenitor in ensembles of mouse embryonic stem cells. *Development* **141**, 4243-4253.

Tzouanacou, E., Wegener, A., Wymeersch, F. J., Wilson, V. and Nicolas, J.-F. (2009). Redefining the progression of lineage segregations during mammalian embryogenesis by clonal analysis. *Dev. Cell* **17**, 365-376.

Whiting, J., Marshall, H., Cook, M., Krumlauf, R., Rigby, P. W., Stott, D. and Allemann, R. K. (1991). Multiple spatially specific enhancers are required to reconstruct the pattern of Hox-2.6 gene expression. *Genes Dev.* **5**, 2048-2059.

Wilson, V. and Beddington, R. S. P. (1996). Cell fate and morphogenetic movement in the late mouse primitive streak. *Mech. Dev.* **55**, 79-89.

Wilson, V., Olivera-Martinez, I. and Storey, K. G. (2009). Stem cells, signals and vertebrate body axis extension. *Development* **136**, 1591-1604.

Yamaguchi, T. P., Takada, S., Yoshikawa, Y., Wu, N. and McMahon, A. P. (1999). T (Brachyury) is a direct target of Wnt3a during paraxial mesoderm specification. *Genes Dev.* **13**, 3185-3190.

Yoshikawa, Y., Fujimori, T., McMahon, A. P. and Takada, S. (1997). Evidence that absence of Wnt-3a signaling promotes neuralization instead of paraxial mesoderm development in the mouse. *Dev. Biol.* **183**, 234-242.

DEVELOPMENT